JOURNAL OF OPTOELECTRONICS AND ADVANCED MATERIALS Vol. 9, No. 7, July 2007, p. 2251 – 2257

Precursor affected properties of nanostructured sulfated zirconia: morphological, textural and structural correlations

G. BOSKOVIC, A.R. ZARUBICA, P. PUTANOV[a]
University of Novi Sad, Faculty of Technology, Cara Lazara 1, 21000 Novi Sad, Serbia
[a]Serbian Academy of Sciences and Arts, Knez Mihajlova 35, 11000 Belgrade, Serbia

Two types of zirconium(IV)-hydroxides were synthesized differing in precursor type and preparation procedure. Impacts of material origin, synthesis parameters, sulfates incorporation, and thermal treatment onto morphological, textural and structural properties of the final material were investigated. Nanosized particles of 10-20 nm in diameter were obtained by sol-gel method when very base conditions were performed, while lowering of pH brings particles of bigger size. Zirconium(IV)-hydroxide of nitrate origin obtained by standard precipitation procedure is attributed with very small particles of nano-dimensions, as well as the highest surface area and the smallest mean pore diameter in series. The main difference between zirconium(IV)-hydroxides obtained from different precursors is in pore-size distribution, which is of bimodal type in the case of zirconium(IV)-hydroxide of alkoxide origin and monomodal class when nitrate was used as the basic material.

(Received April 23, 2007; accepted June 27, 2007)

Keywords: Nanosized sulfated zirconia, Material precursor, Memory effect, Morphology, Structure, Texture

1. Introduction

Zirconium oxide has been utilized in various applications related to its different properties. For example, it has been used as sensor due to its electric conductivity and piezoelectricity, as well as a stabile ceramic material owing to its thermal and mechanical shock resistance and ability of easy incorporation of textural promoters [1].

Zirconia alone or doped with different ions has also been used as efficient catalyst [2-10]. Next to its activity, it is non-corrosive, easily handled and once deactivated the catalyst is environmentally benign and can be easily displaced. Modified with anions such as sulfates, zirconia may exhibit superacidity and could be used in many reactions requiring acidic function [5]. In general, the incorporated anions have stabilization role in zirconia, affecting increase of its thermal stability due to favorable crystal phase composition, and accomplishment of preferred specific surface area and pore size distribution [3,11].

The above-mentioned zirconia properties strongly depend on preparation, differing in methods of synthesis and their parameters leading to various textural, structural and morphological properties. Preparation parameters of real interest are: temperature, pH, concentration of solution, duration of precursor aging, nature of sulfating agent, as well as an order and number of steps in the synthesis sequence [3,6,7]. Synthesis of high-purity nanocrystalline zirconia powder with controlled particle size and morphology is the key factor in achievement of material with favorable properties. Nevertheless, there is still no consensus in correlation of zirconia origin and preparation procedure with its morphological, structural and textural properties.

Sol-gel method based on organic precursor is frequently used for preparation of materials with advantageous properties [9,10,12,13]. The benefits are emphasized through valuable pore structure, which can be tailored due to well-organized particles of nano-size. In addition to common parameters of synthesis from inorganic precursor, sol-gel method requires some additional parameters to be controlled. These are duration of aging of sol, alcohol-alkoxide-water ratio, the choice of solvent, etc., all of them controlling the properties of the resulting product. The proper choice results in nanomaterials characterized by increased homogeneity, defined morphology and thermal stability [14]. On another side, traditional methods of synthesis based on inorganic salts are easier for handling and less sensitive to environment [6,7,15].

The aim of this paper is to investigate morphological, textural and structural properties of sulfates-promoted zirconia as a function of preparation methods and type of precursors.

2. Experimental procedure

Two series of zirconium(IV)-hydroxide (ZH) were prepared from different precursors by related preparation methods, following sulfation and calcination. ZH-N sample, based on nitrate precursor, was prepared from $ZrO(NO_3)_2 \cdot xH_2O$ (Aldrich Co.) by precipitation with 25% NH_4OH at pH=9.5. The obtained hydroxide was filtered, rinsed with distilled water and dried at 110^oC in static conditions for 24 h [6,7]. ZH-A sample, based on alkoxide precursor, was prepared from Zr(IV)-propoxide (70 wt.% solution in 1-propanol) (Aldrich Co.) by mixing two solutions: zirconium(IV)-propoxide in propanol, and

propanol in de-ionized water. Ratio of water to zirconium(IV)-propoxide was 2:1. Solutions were mixed vigorously with magnetic stirrer, in order to obtain zirconia-sol (concentration of 0.5 mol/dm^3), and by adding NH_4OH (25%) the sol was kept at desired pH, which was altered from 9 to 14. The sol was aged for different periods of time (1, 3, 6 or 18 h), centrifuged, rinsed with de-ionised water (8 times) and alcohol, filtered and then dried at 110ºC in static conditions for 24 h [10,12].

The sulfation step of both hydroxides was done by wet-impregnation using 0.5M H_2SO_4 to get nominal sulfates content of 4%. Resulting sulfated zirconium(IV)-hydroxides were calcined at 600^{o}C or 700^{o}C for 3h, with a temperature ramp of 30^{o}C/min and under air flow of 25 cm^3/min. Consequently, several samples were obtained depending on the step in the preparation sequence where they were taken from. They are denoted as follows: ZH (uncalcined Zr(IV)-hydroxide), or Z (zirconia, i.e. Zr(IV)-oxide obtained after the hydroxide calcination), following by letters A or N (depending on the hydroxide precursors – alkoxide, or nitrate), following by numbers: 9, 9.5 or 14 (indicating pH used in the synthesis), further following by numbers: 1, 3, 6 or 18 (denoting time of sol aging in hours). In the case when sulfates were added to the sample letter S appears in the specification, and when calcination was applied additional numbers, 600 or 700, denote the calcination temperature in ^{o}C. Thus, sample ZH-A-14-3 means Zr(IV)-hydroxide obtained from alkoxide at pH=14, following aging of sol for 3 hours, and Z-A-14-3-S-600 is the previous sample after sulfation and following calcination at 600^{o}C. The list of samples together with their textural and structural properties is given in Table 1. For the sake of clarity the samples are also referred by numbers of their appearance in the Table.

Textural characteristics of samples were investigated by means of surface area determined by BET, and main pore diameter and pore volume determined using desorption isotherms. Corresponding data were obtained by dynamic low temperature nitrogen adsorption/desorption (LTNA) using He as carrier gas on Micromeritics ASAP 2010. The crystal structure was resolved by means of X-ray diffraction analysis (XRD) using Philips APD-1700 diffractometer with Cu-anticathode and monochromator, at 40 kV and 55 mA. The crystallite size was estimated from the full width at half-maximum using Scherrer's equation. The prevailing fraction of tetragonal or monoclinic zirconia phase was calculated from diffraction line profiles using corresponding intensities for both phases at angles 2θ = 30.30^o, 2θ = 28.25^o and 31.30^o, respectively [16]. The surface morphology of catalysts samples was investigated by scanning electron microscope (SEM) JEOL JSM-6460LV at accelerating voltage of 25 kV. Solid samples previously were coated with gold in order to achieve their conductivity. To investigate influence of aging of sol on morphology, corresponding samples were prepared by evaporation of drops from equivalent sol solutions deposited directly on the sample-holder grid.

3. Results and discussion

In Fig. 1a and Fig. 1b, SEM pictures of unsulfated zirconium(IV)-hydroxide samples based on different precursors, ZH-N-9.5 (Sample 1) and ZH-A-9-1 (Sample 4) are presented at magnification of 10,000 times. At first glance the basic difference is in more bulky shape of the sample which was obtained from nitrate (Fig. 1a). At the same time the structure of Sample 4 of alkoxide origin looks grainier, and apparently consists of particles of smaller size (Fig. 1b). In the matter of fact, the true is quite opposite, as can be seen in Fig. 1c and Fig. 1d, both obtained using much higher magnification (150,000 times). The basic hydroxide crystallites of nitrate origin consist of very small nano-size particles with diameter of 10-20 nm (Fig. 1c). The corresponding hydroxide crystallites based on alkoxide precursor are, however, at least 5-10 times bigger (Fig. 1d). The particles of different sizes form various pores in ZH: very small particles of the Sample 1 of nitrate origin form pores of almost micro-dimension, i.e. 2.2 nm, as can be seen from Table 1. Consequently, bigger particles of Sample 4 of alkoxide origin in points of their encountering form pores of significantly higher mean diameter, i.e. 3.1 nm. In addition, specific surface area as directly related to pores size is much higher in the case of the Sample 1, thus confirming the previous observation.

An additional difference between various ZH owing to their preparation methods and different precursors is pore size distribution, as shown in Fig. 2. It is of monomodal type when the ZH sample comes from the nitrate precursor (Sample 1), and of bimodal class, with the dominant fraction of mesopores of 30 nm diameter, in the case of the ZH of alkoxide origin (Sample 4). A favorable influence of mesopores on catalytic activity and stability of sulfated ZrO_2 in *n*-paraffin isomerization reaction has been acknowledged earlier [10]. It was attributed to deactivation by coke accumulation occurring by individual sites coverage mechanism in mesopores in contrast to pore blocking mechanism in the case of micropores [17].

The size of crystallites obtained by traditional precipitation method is known to depend on both temperature and concentration of the solution. At high concentration and low temperature plentiful of nucleus are formed resulting in great number of small particles. The following increase of particles size is the result of agglomeration of primary particles [18]. The resulting morphological and textural properties of product including its particles sizes are strongly influenced by ″memory effect″, assuming that the preparation history of the final material affects its properties [19]. It was proved later that ″memory effect″ can be extended to the properties of the parent materials, i.e. precursors used in the synthesis [20]. The last can be understood at least as a part of epitactic or topotactic mechanisms [21].

The previous morphological observations fit perfectly to structural properties of the same materials given in Table 1. Namely, amorphous phases of both ZH-N-9.5 and ZH-A-9-1 are in line with previous claims in literature that phase transformation from amorphous zirconium(IV)-hydroxide to the crystalline tetragonal zirconia phase does not occur before ZH is exposed to calcination at minimal

temperature of 400°C [22]. Although the suggestion on existence of particles of different size based on SEM pictures cannot be proved by XRD due to amorphous structure of ZHs´, Samples 1 and 4, it seems logical in light of their textural properties. Grouping of bigger crystallites of various sizes in the hydroxide of alkoxide origin (ZH-A-9-1) into larger clusters finally forms multimodal pore structure with predominantly wide pores on meso-scale. This scenario consequently ends with higher total pore volume and lower specific surface area in the case of Sample 4 comparing to Sample 1 (Table 1).

Table 1. Textural and structural properties of zirconium(IV)-hydroxide (ZH) and zirconium(IV)-oxide (Z) samples prepared from different precursors.

Sample	Sample No	Surface area, $m^2 \cdot g^{-1}$	Mean pore diameter, nm	Total pore volume, cm^3	Prevailing phase composition	Zirconia crystalline size, nm
ZH-N-9.5	1	283	2.2	0.112	a[1]	/
Z-N-9.5-S-600	2	117	4.4	0.138	t[2]	10.2
Z-N-9.5-S-700	3	89	6.0	0.141	m[3]	12.7
ZH-A-9-1	4	181	3.1	0.162	a	/
ZH-A-14-1	5	170	3.1	0.156	a	/
ZH-A-14-3	6	219	4.0	0.204	a	/
ZH-A-14-6	7	204	3.0	0.174	a	/
ZH-A-14-18	8	191	3.0	0.179	a	/
ZH-A-14-1-S	9	127	3.9	0.169	a	/
ZH-A-14-3-S	10	199	3.1	0.188	a	/
ZH-A-14-18-S	11	69	7.4	0.139	a	/
Z-A-14-3-S-600	12	73	7.2	0.148	t	12.7
Z-A-14-3-S-700	13	65	8.3	0.162	t	14.9
Z-A-9-3-S-600	14	92	5.4	0.176	t	11.7
Z-A-9-3-S-700	15	75	7.5	0.202	m ≈ t	12.7

[1] – amorphous phase; [2] – tetragonal zirconia phase; [3] – monoclinic zirconia phase

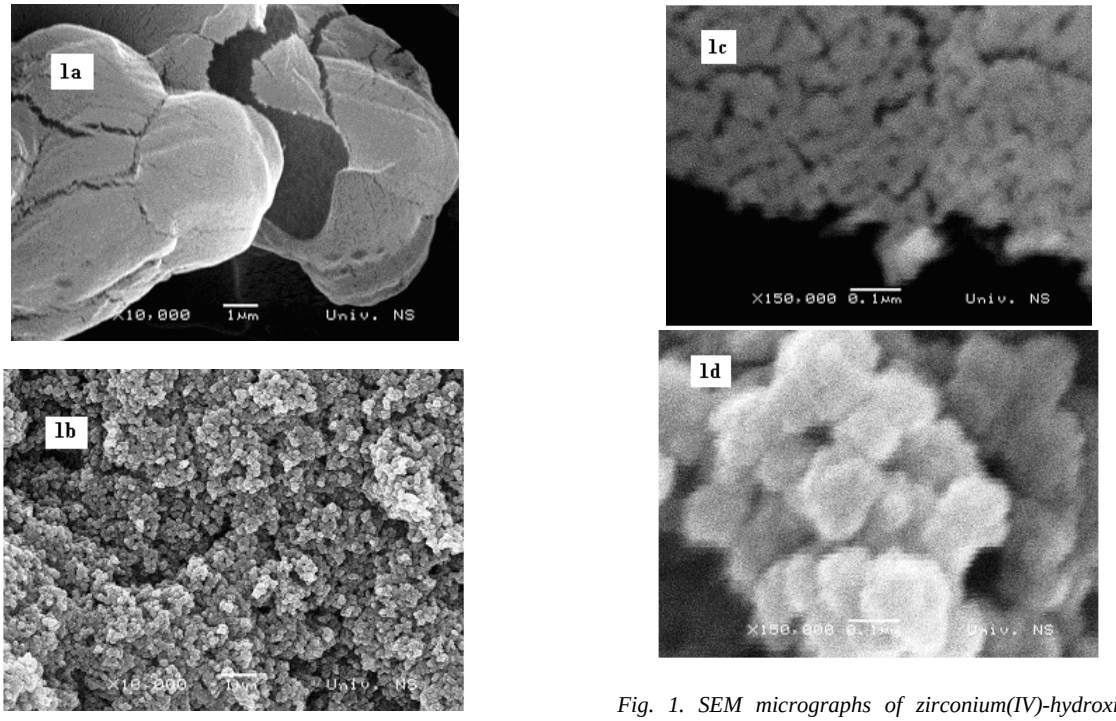

Fig. 1. SEM micrographs of zirconium(IV)-hydroxide samples of different origin: a) ZH-N-9.5 – Sample 1; c) ibid; b) ZH-A-9-1 – Sample 4; d) ibid (notice a difference in magnification).

In Fig. 3, SEM micrographs of four ZH of alkoxide origin obtained at pH=14 but differing in time of aging of sols are presented (Samples 5-8). As expected, in the sol-gel procedure maturing of sol solution is not beneficial for keeping the size of particles small. Namely, polycondensation, which started at certain point has continued to progress, and as a result of networking particles grow their sizes are getting bigger (Fig. 3a vs. Fig. 3b). The resulting pore size for all samples is, however, the same, within the limits of measurements error, with an exception of Sample 6 reaching the maximal value of mean pore diameter in the series (4 nm, Table 1). The corresponding specific surface areas for samples are expected to be inversely proportional to their mean pore diameters. However, as seen by comparing images from Fig. 3 with data from Table 1, the maximal surface area is reached for the sample having the smallest particles (Fig. 3b) but at the same time the largest mean pore diameter in the whole series (Table 1). This speaks of textural properties as a complex function of various physical features, like pores size and pores-size distribution, i.e. fraction of pores of given size in the multimodal distribution, but they are probably the function of shape of pores, as well. Namely, although the mean pore diameter of the sample aged for 3 h (Sample 6) is the largest for the series of samples differing in time of sol aging, fraction of pores of smaller size in bimodal pore distribution of the sample is such that results in the maximal surface area value. Indeed, as seen from Fig. 2, fraction of mesopores in Sample 6, with prevailing diameter of 25 nm, is much smaller than the fraction of pores of smaller size. This is fully opposite to the behavior of other samples in the series. This fact interferes with the maximal total pore volume obtained for the Sample 6, which is in line with its largest specific surface area (Table 1). Further aging of sol leads to additional agglomeration of particles, shifting their size to the level above nano-dimensions (Fig. 3c and Fig. 3d). As seen from Fig. 3a and Fig. 3d the size of some of primary particles in the sol aged for 1 hour is roughly 20 nm and the size of these particles increases even 5-10 times upon aging for additional 17 hours. Although the pore-size distribution keeps its bimodal contour with the time of sol aging, the diameter of the most represented larger pores is continuously shifted to higher values; it is 35 nm and 40 nm for Sample 7 (6 h aging) and Sample 8 (18 h aging), respectively, and consequently specific surface area is shrinking (Table 1).

Very important conclusion can be withdrawn comparing samples of alkoxide origin differing in pH of synthesis procedure (Sample 4 and Sample 5). Namely, it was proved earlier by comparison of SEM images (Fig. 1), the superior nano-sized ZH obtained by precipitation method over its counterpart synthesized by the sol-gel method using pH=9. Now, by comparison of images in Fig. 1d and Fig. 3a (notice a difference in magnification!), it is obvious that very base conditions of sol preparation (pH=14) lead to formation of smaller primary particles, very similar by size to the particles of nano-dimension of nitrate origin. It is to mention, however, that images referring influence of time of sol aging were obtained by SEM measurements of particles at the particular moment of synthesis (samples were prepared by evaporation of drops from corresponding sol-solutions). The resulting materials directed to textural investigation were exposed to previous drying of different sols for 24 h (110^{o}C). As seen from Table 1 and Fig. 2, however, this procedure ends up with just about the same pore-size distribution and specific surface area regardless of the used pH in the synthesis (Samples 4 and 5 at Fig. 2 and Table 1).

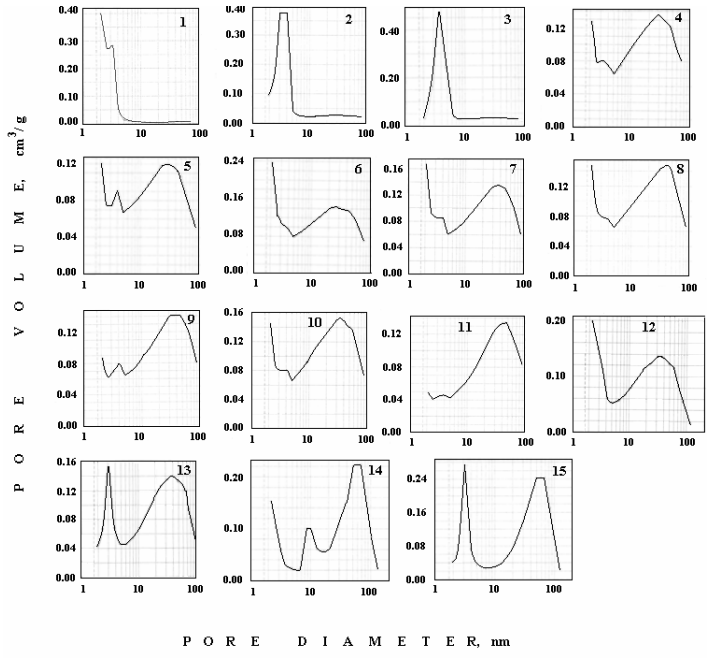

Fig. 2. Pore size distribution and pore volume for different samples.

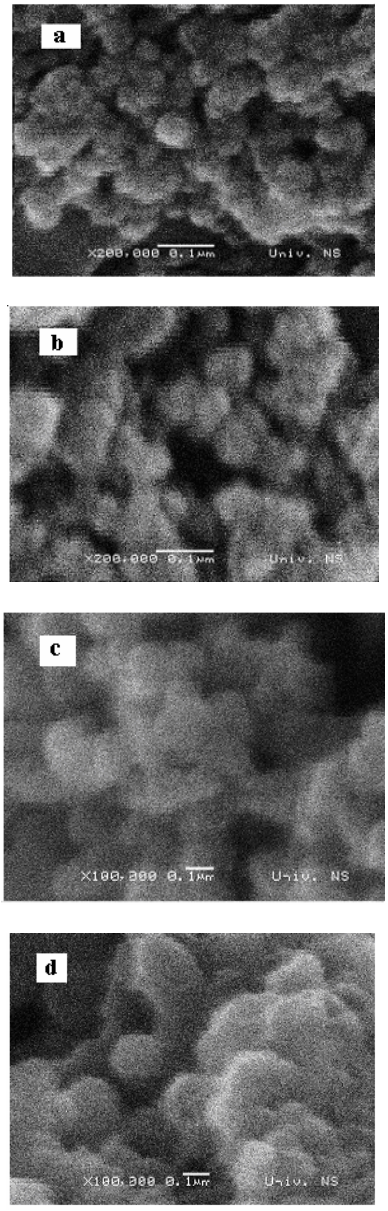

Fig. 3. SEM micrographs of zirconium(IV)-hydroxide samples of alkoxide origin: (pH=14) differing in time of sol maturing: a) 1h; b) 3h; c) 6h; d) 18h (Samples 5-8) (notice a difference in magnification).

Change of morphology and size of samples of alkoxide origin upon sulfates addition and additional thermal treatment is shown in Fig. 4. Introduction of sulfates to ZH brings agglomeration of original grains as seen by comparison of Fig. 4a (Sample 10) and Fig. 3b (Sample 6). This, however, does not bring a big repercussion on textural properties since the specific surface area of sulfated Zr(IV)-hydroxide does not decrease too much in comparison to the unsulfated sample (Table 1). This is in accordance with claims in the literature that incorporation of ions into the Zr(IV)-hydroxide matrix leads to structural and textural stabilization of the host, as well as to the stabilization of the zirconium(IV)-oxide achieved after a thermal treatment of the precursor [11,23]. Further calcination of the sulfated Sample 10 at desired temperatures (Samples 12 and 13) brings particle size agglomeration, mean pore size increase, and consequently specific surface area shrinking, all phenomena linearly increased with calcination temperature increase (Fig. 4 and Table 1). This is in accordance with the data of changing of zirconia crystalline size obtained applying Scherrer's equation based on XRD data (Table 1).

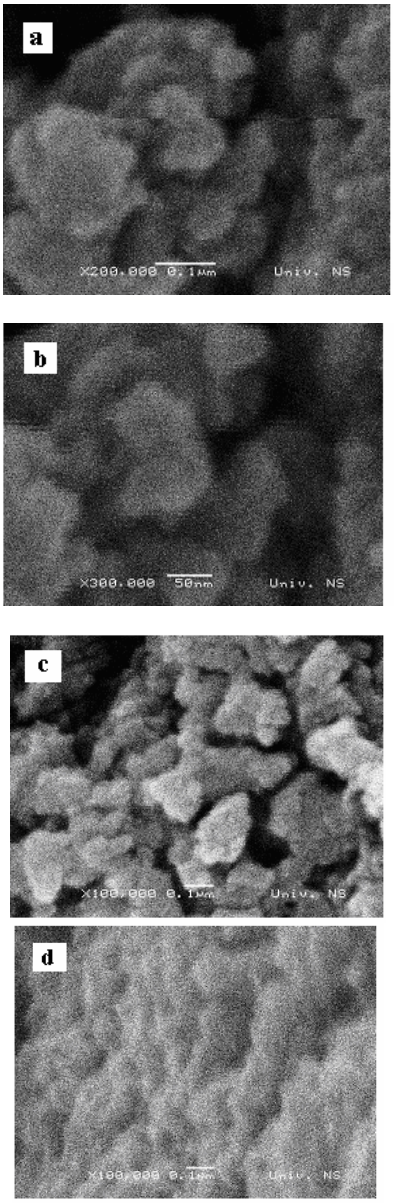

Fig. 4. SEM micrographs of sulfated zirconium(IV)-hydroxide samples of alkoxide origin prepared at pH=14, differing in applied temperature of treatment (a) – sulfated sample aged for 3 h, uncalcined – Sample 10; b) – ibid, different magnification; c) – the same sample calcined at 600 ^{o}C – Sample 12; d) – the same sample calcined at 700 ^{o}C – Sample 13.

The influence of calcination temperature altitude on sulfated samples of different origin is presented in Fig. 5. As seen by comparison of images in Fig. 5a and Fig. 5b with those on Fig. 1c, addition of sulfates to ZH-N-9.5 (Sample 1) and its further temperature treatment is followed by particles agglomeration. Consequently there is an increase of the mean pore size and decrease of surface area (Table 1). Samples of alkoxide origin have exhibited similar behavior, as seen in Fig. 5c and Fig. 5d. According to specific surface area decrease due to calcination (Table 1), it seems, however, that sintering process is somewhat delayed in alkoxide samples obtained using lower pH values. This observation is in line with particles size values calculated by XRD data.

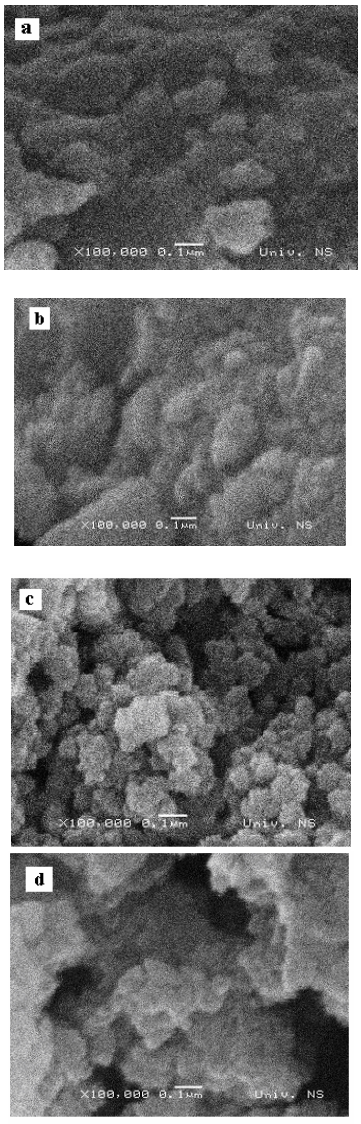

Fig. 5. *SEM micrographs of sulfated zirconium(IV)-hydroxide samples of different origin calcined at various temperatures: a) sulfated ZH-N-9.5 calcined at 600 ^oC - Sample 2; b) sulfated ZH-N-9.5 calcined at 700 ^oC - Sample 3; c) sulfated ZH-A-9-3 calcined at 600 ^oC – Sample 14; d) sulfated ZH-A-9-3 calcined at 700 ^oC – Sample 15.*

4. Conclusions

The preferential smaller size of nano-structured sulfated zirconium(IV)-hydroxide of alkoxide origin is highly affected by pH of the system. Very base conditions of preparation bring particles of nano-size, while by lowering the pH, zirconium(IV)-hydroxide particles 5-10 times bigger in size of previous are obtained. When exposed to calcinations, sintering is delayed in material having bigger particles due to lower degree of interaction among particles. Addition of sulfates brings agglomeration of original particles, as can be observed by SEM, which however does not lead to substantial changes of textural properties. Maturing of sol leads to particle size increase due to polycondensation of initial particles. The size of particles of nano-dimensions is a crucial parameter determining textural properties of the final material. It is, however, the result of synergistic contribution of various physical features, like pores size, pores-size distribution and shape of pores. Precursor properties are highly reflected to pore-size distribution of final materials; it is of monomodal type when zirconium(IV)-hydroxide was obtained from nitrate precursor, and of bimodal character with prevailing fraction of mesopores 30-50 nm in diameter when alkoxide as precursor was used.

Acknowledgment

Financial supports of Serbian Ministry of Science and Environmental Protection (Project ON 142024: “To Green Chemistry via Catalysis”) is highly appreciated.

References

[1] D. Leung, C. Chan, M. Ruhle, F. Lange, J. Am. Chem. Soc. **74**, 2786 (1991).
[2] B. H. Davis, R. A. Keogh, R. Srinivasan, Catal. Today **20**, 219 (1994).
[3] G. D. Yadav, J. J. Nair, Micropor. Mesopor. Mater. **33**, 1 (1991).
[4] J. M. Serra, A. Chica, A. Corma, Appl. Catal. A: General **239**, 35 (2003).
[5] K. Tanabe, T. Yamaguchi, Catal. Today **20**, 185 (1994).
[6] A. Zarubica, M. Kovacevic, P. Putanov, G. Boskovic, XVII International Conference on Chemical Reactors – CHEMREACTOR-17, Athens-Crete, Greece (2006) Book of Abstracts, 81.
[7] A. Zarubica, P. Putanov, G. Boskovic, J. Serb. Chem. Soc., (in press).
[8] G. M. Pajonk, Appl. Catal. **72**, 217 (1991).
[9] C. Breitkopf, A. Garsuch, H. Papp, Appl. Catal. A **296**, 148 (2005).
[10] A. R. Zarubica, M. N. Miljkovic, E. E. Kiss, G. C. Boskovic, React. Kinet. Catal. Lett. **90**, 1, 145 (2007).
[11] M. Benaissa, J. G. Santiesteban, G. Diaz, C. D. Chang, M. J-Yacaman, J. Catal. **161**, 694 (1996).

[12] V. Srdic, R. Djenadic, J. Optoelectron. Adv. Mater. **7** (6) 3005 (2005).
[13] Y. Liu, J. Chen, K. Fang, Y. Wang, Y. Sun, Catal. Commun. **8**, 945 (2007).
[14] M. K. Mishra, B. Tyagi, R. V. Jasra, Ind. Eng. Chem. Res. **42**, 5727 (2003).
[15] N. Nahas, P. Afanasiev, C. Geantet, M. Vrinat, F. Wiss, S. Dahar, J. Catal. **247**, 51 (2007).
[16] H. Toraya, M. Yoshimura, S. Somiya, J. Am. Ceram.Soc. **67**, 119 (1984).
[17] G. Boskovic, M. Baerns, "Catalyst Deactivation" in M. Baerns (Editor): Basic Principles of Applied Catalysis, p.479, Springer-Verlag, Berlin, Heidelberg (2004).
[18] M. Campanati, G. Fornasari, A. Vaccari, Catal. Today **77**, 299 (2003).
[19] B. Delmon, P. Grange in B. Delmon, G. F. Froment (Editors): Catalyst Deactivation, Stud. Surf. Sci. Catal. **6**, 507 (1980).
[20] P. Putanov, E. Kis, G. Boskovic, K. Lazar, Appl. Catal. **73**, 17 (1991).
[21] L. Volpe, M. Boudart, Catal. Rev. - Sci. Eng . **27**, 4, 515 (1985).
[22] T. Yamaguchi, Catal. Today **20**, 198 (1994).
[23] C. J. Norman, P. A. Goulding, I. McAlpine, Catal. Today **20**, 313 (1994).

*Corresponding author: boskovic@uns.ns.ac.yu